Materials Research. 2013; 16(6): 1294-1298
DOI: 10.1590/S1516-14392013005000116

Corrosion Resistance and Glass Forming Ability of $Fe_{47}Co_7Cr_{15}M_9Si_5B_{15}Y_2$ (M=Mo, Nb) Amorphous Alloys

***Carlos Alberto Caldas de Souza*[a]*, *Claudomiro Bolfarini*[b], *Walter José Botta Jr.*[b],**

***Luiz Rogério Pinho de Andrade Lima*[a], *Marcelo Falcão de Oliveira*[c], *Claudio S. Kiminami*[b]**

[a]*Department of Materials Science and Technology, Federal University of Bahia – UFBA, Rua Aristides Novis, 2, CEP 40210-630, Salvador, BA, Brazil*
[b]*Department of Materials Engineering, Federal University of São Carlos – UFSCar, Rod. Washington Luis, Km 235, CEP 13565-905, São Carlos, SP, Brazil*
[c]*Department of Materials Engineering, Aeronautics and Automotive, São Paulo University – USP, Av. Trabalhador São Carlense, 400, Centro, CEP 13566-590, São Carlos, SP, Brazil*

Received: February 8, 2013; Revised: May 15, 2013

In the present work the effect of substituting Mo with Nb on the glass forming ability and corrosion resistance of Fe-Co-Cr-M-Si-B-Y (M=Mo, Nb) ribbons with high corrosion resistance is investigated. The X-ray powder diffraction pattern indicates that the alloy containing both Nb and Mo presented greater glass forming ability than the alloy containing either of these elements separately. The results obtained indicate that Mo is more effective in enhancing corrosion resistance than the Nb in 4.0 M HCl solution. The alloy containing both Nb and Mo presented greater overall corrosion resistance than the alloy containing only one of these elements.

Keywords: *amorphous alloys; corrosion; glass forming ability*

1. Introduction

The presence of a higher molybdenum content in Fe-based amorphous alloys enables the production of nickel free alloys with a high corrosion resistance. This is important due to the fact that nickel released as a result of wear or corrosion may cause environmental and health concerns[1,2].

In recent studies[3] it has been reported that a Fe-based bulk metallic glass (BMG) ($Fe_{41}Co_7Cr_{15}Mo_{14}C_{15}B_6Y_2$) with a diameter of 5mm exhibits high corrosion resistance in simulated body fluids. However, the commercial application of Fe-based bulk metallic glass with a high Mo content is expensive. Therefore it is important to carry out studies to analyze the effect of Mo substitution with other elements for corrosion resistance and glass forming ability. BMG with the greatest corrosion resistance should have a high glass forming ability (GFA), because it has to have a big enough diameter for use in applications such as medical implants. Therefore a study of these alloys should analyze the effect of alloying elements on the GFA.

It has been reported in the literature that the addition of Nb to Fe-Cr-Mo based amorphous alloys is effective in enhancing corrosion resistance. The addition of 2% Nb to an Fe-Cr-Mo-(Nb)-C-B alloy ($Fe_{45}Cr_{16}Mo_{16}C_{18}B_5$ and $Fe_{45}Cr_{16}Mo_{14}Nb_2C_{18}B_5$) is effective in enhancing the corrosion resistance in HCl solution[4] and that an alloy containing both Nb and Mo (0.15 wt.% Mo and 0.15 wt.% Mo) presented greater corrosion resistance than an alloy containing only Mo (0.15 wt.% Mo) in HCl and H_2SO_4 solution[5]. However, the effect of Mo compared to Nb on the corrosion resistance of alloys that present a typical composition of BMG with high corrosion resistance is not clear. Moreover, the effect of Mo compared with Nb on the GFA of these BMGs is not clear.

Si has been added to several Fe-based BMGs such as $Fe_{57.6}C_{7.1}Si_{3.3}B_{5.5}P_{8.7}Cr_{12.3}Mo_{2.5}Al_{2.0}Co_{1.0}$ [6] and $Fe_{59.1}C_{7.1}Si_{4.4}B_{6.5}P_{8.6}Cr_{12.3}Al_{2.0}$ [7]. In the latter alloy, it was found that the Si content is high enough to form SiO_2 phases in the passive film which promotes corrosion resistance.

A possible approach to investigate the effect of composition on the GFA and the corrosion resistance of BMG is to make amorphous ribbons of different compositions from the melt-spinning technique and then use the results obtained to design a BMG with high corrosion resistance[8]. In the present study the effect of the substitution of Mo with Nb on the glass forming ability and corrosion resistance of $Fe_{47}Co_7Cr_{15}M_9Si_5B_{15}Y_2$(M=Mo,Nb) ribbons alloy is investigated.

2. Experimental Procedure

Ribbons of 20 to 30 μm thick were produced using melt spinning equipment with a copper wheel rotating at a speed of 55 m/s in an argon atmosphere.

The structure of the melt-spun ribbons was characterized by X-ray diffraction (XRD) using Cu-Kα radiation. The thermal stability of the melt spun sample was characterized by differential scanning calorimetry (DSC). The DSC scans were performed under continuous heating from room temperature to 1273 K with a heating rate of 40 K min^{-1}.

*e-mail: caldassouza@hotmail.com

The mixing enthalpy values, ΔH, of the alloys analyzed were obtained from the mixing enthalpies of atomic pairs among the elements present in the alloy[9]. The ΔH values of the alloys were calculated considering the stoichiometry of the alloy. To perform these calculations we used the software MSExel.

Corrosion resistance was evaluated by weight loss corrosion tests and potentiodynamic polarization curves in aerated solutions of 4.0 M HCl at room temperature.

The samples for weight-loss measurements were mechanically ground using emery SiC paper (600 grit). Subsequently, the samples were ultrasonically cleaned in acetone for 5 min, rinsed with distilled water and dried. After their initial weight and surface area were measured, they were immersed in the test solution. After being immersed for 13 hours, the samples were cleaned, rinsed and dried. Subsequently the samples were weighed. For the weight measurements a Mettler AB2004 analytical balance was used. Each test was performed with the samples immersed in the solution and the weight loss corrosion test was repeated three times for each condition.

The polarization curves were carried out at a scan rate of 2 mV/s using the alloy ribbons as the working electrode, which was electrically connected to an isolated wire. The auxiliary electrode was a graphite cylinder, and a saturated calomel electrode (SCE) was used as reference. Before each experiment, the sample surface was ground with emery SiC paper (600 grit). A potenciostat-galvanostat AUTOLAB model PGSTAT 100 was used.

3. Results and Discussion

3.1. *Glass forming ability*

Figure 1 shows the XRD patterns of the as-cast melt spun ribbons. For $Fe_{47}Co_7Cr_{15}Mo_{4.5}Nb_{4.5}Si_5B_{15}Y_2$ ribbon alloy, as shown in this figure, there is one diffuse intensity peak indicating the formation of an amorphous structure. However, for alloys containing only Nb or Mo, as well as the diffuse intensity peak, there is also the presence of several sharp Bragg peaks, indicating the presence of crystalline phases. Therefore, according to the XDR obtained, the alloy containing both Nb and Mo presented greater glass forming ability than the alloy containing either of these elements.

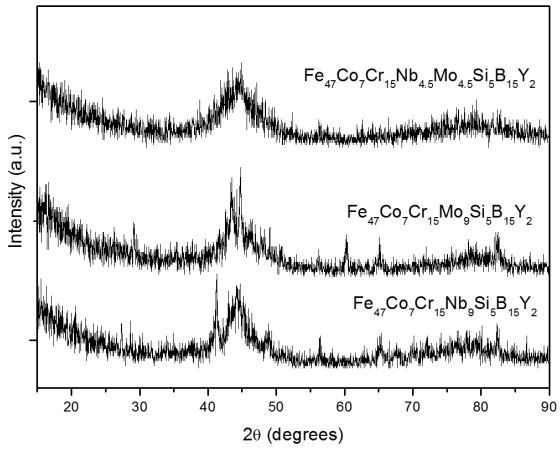

Figure 1. XRD patterns of as-cast alloys.

The glass forming ability, GFA, is a function of liquid phase stability and crystalline resistance[8]. The high supercooled liquid region results in low temperature nucleation, therefore the nucleation kinetics of the crystalline phase is inhibited. The high supercooled liquid region is a consequence of the formation of a highly dense random packed structure[10], which occurs when three empirical rules are satisfied: (1) multi-component alloy systems consist of more than three elements, (2) significantly different atomic radius ratios above about 12% among the main constituent elements are present, and (3) the heats of mixing among their elements are negative. More negative values of mixing enthalpies of atomic par make the bonding nature stronger between these atoms, which results in increased GFA. In the present paper the effect of composition on the GFA of alloys analyzed is discussed in the framework of these three empirical rules.

The atomic radius of the elements Nb and Mo and their difference from the atomic radius of Fe are listed in Table 1. The difference in the atomic radius of Nb with Fe is the greatest. The greater different atomic size ratios among the main constituent elements lead to more efficient packing, thus stabilizing the liquid stability, which favors GFA[10]. Therefore, because of the atomic size difference the addition of Nb to Mo can improve the GFA. A larger number of alloying elements could lead to an increase in GFA because the tendency of forming all crystalline phases can be difficult. Thus, from this point of view the addition of Nb to Mo could also improve the GFA.

Table 2 shows the mixing enthalpy values, ΔH, of the alloys analyzed. The $Fe_{47}Co_7Cr_{15}Mo_{4.5}Nb_{4.5}Si_5B_{15}Y_2$ alloy presents a higher negative value of ΔH in comparison with the $Fe_{47}Co_7Cr_{15}Mo_9Si_5B_{15}Y_2$ alloy, which is coherent with the higher GFA of the alloy containing Nb and Mo. However, the alloy containing only Nb, despite having more negative values of mixing enthalpies compared to the other alloys, has a lower GFA in comparison with the alloys containing Nb and Mo. Therefore, this indicates that as well as the three empirical rules which are related to the liquid phase stability, there are other factors that affect the stability of the alloys analyzed related to the crystalline resistance.

Table 1. Atomic radius of the elements (r_{Mo}, r_{Nb}, r_{Fe}) and the atomic size mismatch with the Fe atomic radius.

r_{Mo} (Å)	$(r_{Fe} - r_{Mo})/r_{Fe}$ (%)	r_{Nb} (Å)	$(r_{Fe} - r_{Nb})/r_{Fe}$ (%)
1.360	9.6	1.429	15.1

Table 2. Mixing enthalpies values of alloys, ΔH.

Alloy	ΔH (kJ/mol)
$Fe_{47}Co_7Cr_{15}Mo_9Si_5B_{15}Y_2$	–17.8
$Fe_{47}Co_7Cr_{15}Nb_9Si_5B_{15}Y_2$	–22.7
$Fe_{47}Co_7Cr_{15}Mo_{4.5}Nb_{4.5}Si_5B_{15}Y_2$	–20.5

To compare the GFA of $Fe_{47}Co_7Cr_{15}Mo_{4.5}Nb_{4.5}Si_5B_{15}Y_2$ alloy with amorphous alloys obtained as BMG cited in literature, the DSC curve of this alloy was obtained. Figure 2 shows the DSC curve of the $Fe_{47}Co_7Cr_{15}Mo_{4.5}Nb_{4.5}Si_5B_{15}Y_2$ amorphous ribbon. The presence of a glass transition temperature, T_g, characterizes this sample as a "glassy metallic alloy". Apart from T_g, the temperature of crystallization, T_x, and the liquidus temperature, T_l, are given in Table 3, where the γ parameter corresponds to the relationship between T_x and T_g+T_l. This table also shows the values of T_g, T_x, T_l, and the γ of BMG, cited in literature[3,11,12] which has a thickness greater than 1mm. The γ parameter is effective in evaluating the GFA because it incorporates both the liquid phase stability and the crystalline resistance effects[8]. It can also be seen in Table 3 that the γ parameter of the $Fe_{47}Co_7Cr_{15}Mo_{4.5}Nb_{4.5}Si_5B_{15}Y_2$ alloy is higher than several alloys which are obtained as BMG[3,11,12]. In future studies the making of $Fe_{47}Co_7Cr_{15}Mo_{4.5}Nb_{4.5}Si_5B_{15}Y_2$ alloy as BMG will be investigated.

3.2. *Corrosion resistance*

The effect of substituting Mo with Nb on the corrosion resistance of the alloys was evaluated from mass loss measurements. The results, which were obtained in 4.0 M HCl aerated solution, are shown in Table 4.

The results obtained from mass loss indicate that the alloy containing Mo presented a more uniform corrosion resistance than the alloy containing Nb. However, the highest corrosion resistance was observed in the alloy containing both Nb and Mo in relation to the alloy containing either of these elements alone.

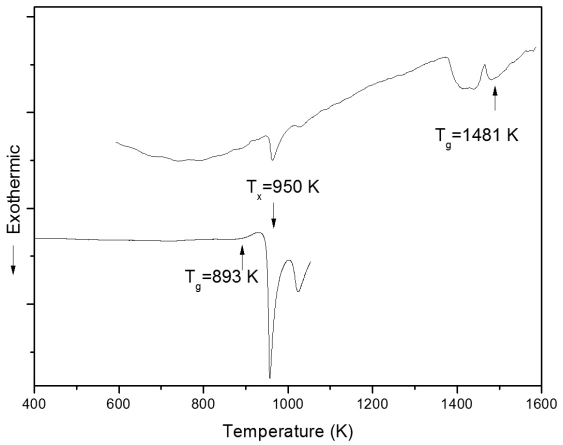

Figure 2. DSC Thermograms of $Fe_{47}Co_7Cr_{15}Mo_{4.5}Nb_{4.5}Si_5B_{15}Y_2$ amorphous sample obtained at heating rates of 40 K/min.

Table 3. The glass transition temperature, T_g, onset of crystallization temperatures, T_x, liquidus temperature, T_l, and γ parameter of different glass metallic alloys.

Alloy	T_x(K)	T_g(K)	T_l(K)	$\gamma=T_x/Tg+T_1$
$Fe_{48}Cr_{15}Mo_{14}Y_2C_{15}B_6$ [11]	896	848	1548	0.374
$(Fe_{69}Mn_{26}Cr_5)_{0.68}Zr_4Nb_4B_{24}$ [12]	971	886	1413	0.422
$Fe_{41}Co_7Cr_{15}Mo_{14}C_{15}B_6Y_2$ [3]	876	838	1437	0.385
$Fe_{47}Co_7Cr_{15}Mo_{4.5}Nb_{4.5}Si_5B_{15}Y_2$	950	893	1481	0.400

Figure 3 shows the potentiodynamic polarization curves of the as-cast alloy in 4.0 M HCl solution. Note that under an applied potential larger than a value about 0.1 V vsHg/Hg_2Cl_2, the current density of the alloy shows a slight variation with potential, which indicates the formation of a passive film. The lower values of current density in passive region, i_p, are related to a higher protective capacity of the passive film. The alloys have different current density values in passive region passivity, i_p, indicating that the passive film of these alloys exhibits different protective ability against corrosion. The i_p values indicate that in relation to the protective ability of the passive film, the alloys can be put in the following ascending order: $Fe_{47}Co_7Cr_{15}Nb_9Si_5B_{15}Y_2$, $Fe_{47}Co_7Cr_{15}Mo_9Si_5B_{15}Y_2$ and $Fe_{47}Co_7Cr_{15}Mo_{4.5}Nb_{4.5}Si_5B_{15}Y_2$, alloys. These results are consistent with measures of loss mass indicating that the corrosion resistance of the alloys analyzed is related to the protective ability of the passive film.

Table 5 shows the corrosion potential, E_{cor}, of as cast alloys obtained from Figure 3. The highest corrosion potential of the alloy contain Nb and Mo, indicating a higher corrosion resistance of this alloy, while the lowest corrosion potential of the alloy contains only Nb which indicates the lower corrosion resistance of this alloy.

The high corrosion resistance of Fe-Cr based amorphous alloys is usually attributed to the formation of the passive film composed mainly of chromium-enriched oxyhydroxide. The effect of other alloying elements such Mo and Nb on corrosion resistance is related to the behavior of chromium-enriched oxyhydroxide film or with the formation of another film.

The effect of Nb in enhancing the corrosion resistance can be attributed to the presence of Nb_2O_5 in the passive film. The presence of this oxide, which was detected by XPS analysis of the passive film in FeNbZrCuB amorphous alloy[13], increases the susceptibility to passivation and the protective capacity of passive film. In a Fe-Cr based amorphous alloy immersed in 1 M HCl open to air it was found[14] that the addition of Mo promotes the enrichment of the chromium ion in the film greatly. Furthermore, it has been observed that[15] in 6M HCl solution the addition of Mo promotes the corrosion resistance of glassy Fe–Cr based alloys by the formation of Mo oxide film.

The results obtained in this work indicate that the presence of Mo was more favorable than that of Nb for the passivation and inhibition of corrosion in the HCl solution analyzed. However, in presence of both Mo and Nb the corrosion resistance of the alloy is higher than the alloy content only Mo, suggesting a synergetic effect between these elements.

It has been reported[16] for 30Cr-2Mo ferritic stainless steel in HCl solution that in the passive region the inner MoO_2 film is protected by the outer chromium-enriched oxyhydroxide film. This outer film inhibits the dissolution of Mo, and the MoO_2 film acts as an effective barrier against the diffusion of matter through the film. Therefore it is possible that the presence of Nb_2O_5 has the effect of increasing the protective capacity of the outer film and decreasing the active dissolution of the MoO_2 film. However, the occurrence of

Table 4. Mass losses resulting of as cast alloys immersed in 4M HCl.

Alloy	Immersion time	Mass losses	Surface area	Mass losses /Surface area	
	(hours)	(g)	(mm^2)	Mean Value ($x\ 10^{-5}\ g/mm^2$)	Standard Deviation ($x\ 10^{-5}\ g/mm^2$)
$Fe_{47}Co_7Cr_{15}Nb_{9.0}Si_5B_{15}Y_2$	13	0.0012 0.0006 0.0008	12.62 11.97 11.85	7.09	2.27
$Fe_{47}Co_7Cr_{15}Mo_9Si_5B_{15}Y_2$	13	0.0005 0.0004 0.0004	11.79 13.11 12.68	3.58	0.84
$Fe_{47}Co_7Cr_{15}Mo_{4.5}Nb_{4.5}Si_5B_{15}Y_2$	13	0.0003 0.0002 0.0002	12.50 11.06 11.85	2.06	0.48

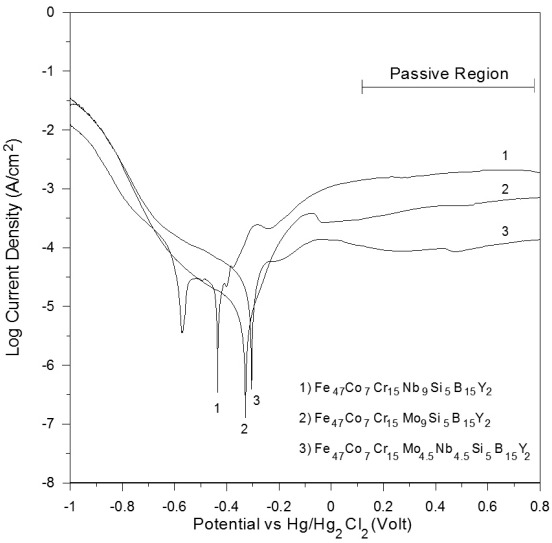

Figure 3. Potentiodynamic polarization curves of as-cast alloys in 4M HCl solution open to air, obtained at a scanning rate of 2 mVs^{-1}.

this behavior for amorphous Fe-Cr based alloys should be evaluated using surface analysis techniques.

It is also possible that the presence of a crystalline phase in samples containing only Mo or Nb affects the corrosion resistance of these alloys. The presence of a crystalline phase in an amorphous matrix can result in the occurrence of galvanic corrosion between these phases. The presence of galvanic corrosion decreases the corrosion resistance in relation to the sample containing Mo and Nb. However, in order to identify the presence of galvanic corrosion it is necessary to determine the composition and the fraction of the crystalline phase. In previous work[17] it was found that the partially crystalline structure favors Si diffusion resulting in a more protective SiO_2 passive film. Therefore it is possible that the partially crystallization has a positive effect on the corrosion resistance. The composition, the fraction of crystalline phase and the effect of crystallization on the Si diffusion will be evaluated in future work.

Table 5. Corrosion Potential, E_{cor}, of as cast alloys in 4M HCl solution.

Alloy	E_{cor} (V)
$Fe_{47}Co_7Cr_{15}Mo_9Si_5B_{15}Y_2$	–0.328
$Fe_{47}Co_7Cr_{15}Nb_9Si_5B_{15}Y_2$	–0.435
$Fe_{47}Co_7Cr_{15}Mo_{4.5}Nb_{4.5}Si_5B_{15}Y_2$	–0.307

4. Conclusions

In the present paper $Fe_{47}Co_7Cr_{15}M_9Si_5B_{15}Y_2$(M=Mo,Nb) ribbons were obtained. The XDR pattern indicates that the alloy containing both Nb and Mo presents a greater glass forming ability than the alloy containing either of these elements. The presence of these two elements causes the alloy $Fe_{47}Co_7Cr_{15}Mo_{4.5}Nb_{4.5}Si_5B_{15}Y_2$ to exhibit an amorphous structure and high glass forming ability. The results indicate that in the alloys analyzed Mo is more effective in corrosion resistance than Nb in 4.0 M HCl solution. However, the alloy containing both Nb and Mo presents a greater overall corrosion resistance than the alloys containing either of these elements alone.

References

1. Ruff CA and Belsito DV. The impact of various patient factors on contact allergy to nickel, cobalt, and chromate. *Journal of the American Academy of Dermatology*. 2006; 55:32-39. PMid:16781289. http://dx.doi.org/10.1016/j.jaad.2006.04.015
2. Bal W, Kozøowski H and Kasprzak KS. Molecular models in nickel carcinogenesis. *Journal of Inorganic Bichemistry*. 2000; 76:213-218. http://dx.doi.org/10.1016/S0162-0134(99)00169-5
3. Wang YB, Li HF, Cheng, Wei SC and Zheng YF. Corrosion performances of a Nickel-free Fe-based bulk metallic glass in simulated body fluids. *Electrochemistry Communications*. 2009; 11:2187-2190. http://dx.doi.org/10.1016/j.elecom.2009.09.027
4. Pang SJ, Zhang T, Asami K and Inoue A. New Fe-Cr-M0-(Nb,Ta)-C-B. Glassy Alloys with High Glass-Forming Ability and Good Corrosion Resistance. *Materials Transactions Japan Institute of Metals*. 2001; 42:376-379.

5. Kiminami CS, Souza CAC, De Andrade LRP, Surinach S, Baro MD, Bolfarini C et al. Partial crystallization and corrosion resistance of amorphous Fe-Cr-M-B (M = Mo, Nb) alloys. *Journal of Non-Crystalline Solids*. 2010; 356:2651. http://dx.doi.org/10.1016/j.jnoncrysol.2010.04.051
6. Wang SL, Li HX, Zhang XF and Yi S. Effects of Cr contents in Fe-based bulk metallic glasses on the glass forming ability and the corrosion resistance. *Materials Chemistry and Physics*. 2009;113:878-883. http://dx.doi.org/10.1016/j.matchemphys.2008.08.057
7. Wang SL and Yi S. The corrosion behaviors of Fe-based bulk metallic glasses in a sulfuric solution at 70 °C, *Intermetallics*. 2010;18:1950-1953. http://dx.doi.org/10.1016/j.intermet.2010.01.020
8. Lu ZP, Liu Y and Liu CT. Evaluation of Glass-Forming Ability. In: Bulk Metallic Glasses. Burlington: Elsevier; 2006.
9. Inoue A and Takeuchi. Mixing enthalpy of liquid phase calculated by miedemas's scheme and approximated with sub-regular solution model for assessing forming ability of amorphous and glassy alloys. *Intermetallics*. 2010; 18:1779-1789. http://dx.doi.org/10.1016/j.intermet.2010.06.003
10. Ma LA and Inoue A. On glass-forming ability of Fe-based amorphous alloys. *Materials Letters*.1999; 38:58-61. http://dx.doi.org/10.1016/S0167-577X(98)00132-3
11. Hidal K, Sekido N and Perepezko JH. Critical coocling rate for $Fe_{48}Cr_{15}Mo_{14}Y_2C_{15}B_6$ bulk metallic glass formation. Intermetallics. 2006; 14:898-902. http://dx.doi.org/10.1016/j.intermet.2006.01.036
12. Ponnambalam V, Poon SJ, Shifet GJ, Keppens VM, Taylor R and Petculescu G. Synthesis of Bulk Metallic Glasses as Nonferromagnetic Amorphous Steel Alloys. *Applied Physics Letters*. 2003;83:1131-1133. http://dx.doi.org/10.1063/1.1599636
13. Souza CAC, De Oliveira MF, May JE, Botta FWJ, Mariano NA, Kuri SE et al. Corrosion resistance of amorphous and nanocrystalline Fe-M-B (M=Zr, Nb) alloys. *Journal Non Crystalline solids*. 2000; 273:282-288. http://dx.doi.org/10.1016/S0022-3093(00)00174-5
14. Tan MW, Akiyma E, Kawashima A, Asami K and Hashimoto K. The effect of air exposure on the corrosion behavior of amorphous Fe-8Cr-Mo-13P-7C Alloys in 1M HCl. *Corrosion Science*. 1995; 37:1289-1301. http://dx.doi.org/10.1016/0010-938X(95)00035-I
15. Asami K, Naka M, Hashimoto K and Masumoto T. Effect of molybdenum on the anodic behavior of amorphous Fe-Cr-Mo-B alloys in hydrochlori-acid. *Journal Electrochemical Society*. 1980;127:2130-2138. http://dx.doi.org/10.1149/1.2129359
16. Hashimoto K, Asami K, Kawashima A, Habazaki H and Akiyama E.The role of corrosion-resistant alloying elements in passivity. *Corrosion Science*. 2007; 49:42-52. http://dx.doi.org/10.1016/j.corsci.2006.05.003
17. Souza CAC, Kuri SE, Politti FS, May JE and Kiminami CS. Corrosion resistance of amorphous and polycrystalline FeCuNbSiB alloys in sulphuric acid solution. *Journal Non Crystalline solids*. 1999; 247:69-73. http://dx.doi.org/10.1016/S0022-3093(99)00034-4